



ARTICLE

# Nitrogen-Doped Amorphous Carbon Homojunction from Palmyra Sugar as a Renewable Solar Cell

Budhi Priyanto<sup>1,2,\*</sup>, Imam Khambali<sup>1,2</sup>, Irma Septi Ardiani<sup>2</sup>, Khoirotnun Nadhiyah<sup>2</sup>, Anna Zakiyatul Laila<sup>2</sup>, M. Chasrun Hasani<sup>1</sup>, Bima Romadhon<sup>3</sup>, Retno Asih<sup>2</sup>, Yoyok Cahyono<sup>2</sup>, Triwikantoro<sup>2</sup> and Darminto<sup>2,\*</sup>

<sup>1</sup>Department of Electronic Engineering, Faculty of Engineering, Universitas Muhammadiyah Malang, Kota Malang, Indonesia

<sup>2</sup>Advanced Materials Research Group, Department of Physics, Faculty of Science and Data Analytics, Institut Teknologi Sepuluh Nopember, Surabaya, Indonesia

<sup>3</sup>Department of Electronic Engineering, Faculty of Industrials Engineering, Institut Teknologi National Malang, Kota Malang, Indonesia

\*Corresponding Authors: Budhi Priyanto. Email: budhip67@gmail.com; Darminto. Email: darminto@physics.its.ac.id

Received: 29 December 2022 Accepted: 09 June 2023 Published: 23 January 2024

## ABSTRACT

An *a-C/a-C:N* junction, which used palmyra sugar as the carbon source and ammonium hydroxide ( $\text{NH}_4\text{OH}$ ) as the dopant source, was successfully deposited on the ITO glass substrate using the nano-spraying method. The current-voltage relationship of the junction was found to be a Schottky-like contact, and therefore the junction shows the characteristic rectifiers. This means the *a-C* and *a-C:N* are semiconductors with different types of conduction. Moreover, the samples showed an increase in current and voltage value when exposed to visible light (bright state) compared to the dark condition, thereby, indicating the creation of electron-hole pairs during the exposure. It was also discovered that the relationship between current and voltage for the *a-C/a-C:N* junction sample formed a curve that satisfies the rule of the photovoltaic effect when exposed to visible light from a light bulb. The exposure of this sample to direct sunlight at AM 1.5 conditions produced a curve that meets the rules for the emergence of the photovoltaic effect with higher characteristics for the current-voltage relationship. Thus, the *a-C/a-C:N* junction sample is a solar cell successfully fabricated using a sample method and has a maximum efficiency of 0.0013%.

## KEYWORDS

Solar cell; amorphous carbon; palmyra sugar

## 1 Introduction

Carbon is one of the elements in group IV besides silicon. Although in the same group, it differs from silicon in hybridization. Silicon has a single hybridization, namely  $\text{sp}^3$ , while carbon has three hybridizations, namely  $\text{sp}^3$ ,  $\text{sp}^2$  and  $\text{sp}$ . Carbon with 100%  $\text{sp}^3$  hybridization is known as diamond like carbon (*DLC*) and acts as an insulator. Carbon with 100%  $\text{sp}^2$  hybridization is known as graphite and is an excellent conductor. Carbon with mixed  $\text{sp}^3$  and  $\text{sp}^2$  hybridization is known as amorphous carbon. The percentage of carbon hybridization is strongly influenced by its hydrogen content, the deposition parameter and the raw



materials of the carbon source. In this various hybridization, carbon compounds may have various energy gaps in the range of 0 to 6 eV [1,2].

Thin Carbon films are generally deposited using the *Chemical Vapor Deposition (CVD)* method with hydrocarbon compounds as the precursors, such as ethanol [3], methane gas [4–8], di-iso-propyl-ether (*(i-C<sub>3</sub>H<sub>7</sub>)<sub>2</sub>O*) [9], acetylene [10]. The percentage of  $sp^3$ ,  $sp^2$  and  $sp$  hybridization is strongly influenced by the carbon source. Methane gas sources provide a higher percentage of  $sp^3$  than acetylene. The percentage of  $sp^2$  is higher when an acetylene source is used. Diamond like carbon (*DLC*) deposited using a methane gas source is more insulating than that from an acetylene source [11].

Amorphous carbon thin films have been successfully prepared using the CVD method from biomass sources. These films sourced from palm oil have been successfully deposited on glass and p-type silicon [12]. Nitrogen-doped amorphous carbon thin films with ethanol as the source and nitrogen gas as the doping source have been successfully deposited on a p-type silicon substrate [13]. One of the deposition methods besides CVD to prepare amorphous carbon thin films is the spin coating method. Has been successfully deposited using the spin coating method of amorphous carbon thin film with biomass sources (coconut sugar, palmyra sugar, palm sugar and brown sugar), which are deposited on ITO glass substrate. The percentage value of  $sp^2$  hybridization is above 60%, and the value can be adjusted by adjusting the heating temperature of the carbon source. The electrical conductivity values of the amorphous carbon thin films formed are within the range of the electrical conductivity values of semiconductor materials [14–16].

Carbon is a material with great potential for the development of photovoltaic cells. Amorphous carbon absorbs much higher sunlight of sunlight than amorphous silicon at the same thickness [17]. Its high absorption of sunlight provides the potential for carbon applications such as an anti-reflective coating in silicon solar cells [18,19]. Polymeric-like carbon (*PLC*) and *DLC* deposited using *CVD* have been applied as anti-reflective coatings for crystalline silicon solar cells [20]. The extraordinary electronic properties of carbon make it an important component in the development of solar cells. Because of its high electrical conductivity, carbon is used as a back contact in perovskite solar cells [21]. Due to the high electrical conductivity of carbon, it is used as an electrode in perovskite solar cells [22].

Carbon-based solar cells that have been developed previously are generally a heterojunction between carbon and silicon. The carbon source comes from hydrocarbon compounds, and the deposition process uses the (*CVD*) method. Carbon-based solar cells have been successfully made using *SWCVD* with an acetylene source and trimethyl boron as a doping source for a p-type layer. The samples were deposited on an n-type silicon substrate in two *p-C/n-Si* and *p-C/i-C/n-Si* configurations [23]. Using *rf-PECVD*, a solar cell with the *p-PAC/i-a-Si:H/n-Si:H* configurations has been successfully fabricated [24]. Using *AACVD*, carbon-based solar cells have been successfully made with camphor oil as a source. Solar cell samples were made in *Au/p-C/n-Si/Au* configuration [25]. Using *AACVD* with camphor oil sources, heterojunction solar cells with *Au/n-C:N/p-Si/Au* and *Au/a-C/p-Si/Au* configuration have been successfully fabricated. Nitrogen gas is used as a doping source. A Solar cell sample with *Au/a-C/p-Si/Au* configuration when measured using a PV simulator at *AM 1.5* condition obtained an efficiency of 0.000048% [26]. Carbon nanomaterials were integrated with silicon solar cells to form a *CNT-Si* configuration [27]. Carbon-derived homojunction solar cells with *a-C/fullerene(C<sub>60</sub>)* configuration [28,29]. So far, carbon-based solar cells have been dominated by a carbon-silicon heterojunction. Amorphous carbon homojunction solar cells have not yet been developed by previous researchers. The main source of doping in the development of solar cells are gaseous doping sources [12,13,23,25,26], and liquid doping sources have never been used. The main source of carbon as active material is dominated by hydrocarbon compounds, and the use of carbon derived from agricultural products (biomass) has not been significantly developed. The deposition method is dominated by *CVD* and other deposition methods have not been developed for the carbon-based solar cells.

In this research, amorphous carbon thin film deposition has been carried out with a new method that has not been carried out by previous researchers, namely the nano-spraying method. These thin films of amorphous carbon cover boron-doped amorphous carbon and nitrogen-doped amorphous carbon on ITO glass substrates using the nano-spraying method have been successfully prepared with palmyra sugar as a carbon source. The carbon thin film that has been successfully deposited has a smooth, uniform, thin surface (one hundred nanometer), and has good transmission of visible light and infrared.

This paper reports the results of the research on the development of amorphous carbon-based solar cells. The solar cell sample is an amorphous carbon homojunction, which has never been done by previous researchers. The deposition method uses nano-spraying, which has never been done in the development of solar cell technology. The carbon source uses palmyra sugar, which is an agricultural product, available all year round and is renewable, abundant and very cheap. The doping process uses a liquid ammonium hydroxide ( $NH_4OH$ ) source. The results of measuring the electrical conductivity of each layer using a four-point probe, the optical energy gap using UV-Vis spectroscopy, and *PES* testing to determine the occurrence of the doping process included. The results of current and voltage measurements indicate that the sample junction function as a rectifier and as a photovoltaic cell.

## 2 Experiment

### 2.1 Film Deposition

Palmyra sap contains an element *C* of 61.9%, *O* of 35.84%, *Cl* of 0.68%, *Na* of 0.81%, *K* of 0.41%, *P* of 0.18%, *S* of 0.06% and *Si* of 0.01%, which is very good for use as a natural carbon source. The sap is produced from palmyra trees (Fig. 1a) by pruning the flowers that have not yet bloomed. The water that oozes out of the flower stalk is the sap. The sap from the stalk is collected in a vessel. When the volume of the sap has reached a sufficient amount, it is processed to become dilute sugar. The sap that is sufficient must be immediately processed to diluted sugar so that it is not decay. It is heated in open air and stirred so that the evaporation occurs as expected. When the water content is reduced as expected, the cooling process is carried out until it becomes diluted sugar. This process is carried out by farmers in the Palmyra plantation. The yellowish diluted sugar produced from the Palmyra plantation is heated using a hotplate at a temperature of 100°C and stirred with a magnetic stirrer within 120 min to reduce water content. Cooling is done to get dark brown thick sugar (Fig. 1b). Further heating is carried out using a furnace at a temperature of 250°C for 150 min, and cooling is carried out in the furnace. This process produces a very light, shiny black charcoal. The charcoal is washed with distilled water and filtered using paper to remove the potassium chloride (*KCl*) content. The dry charcoal is crushed until very fine powdered charcoal is obtained.

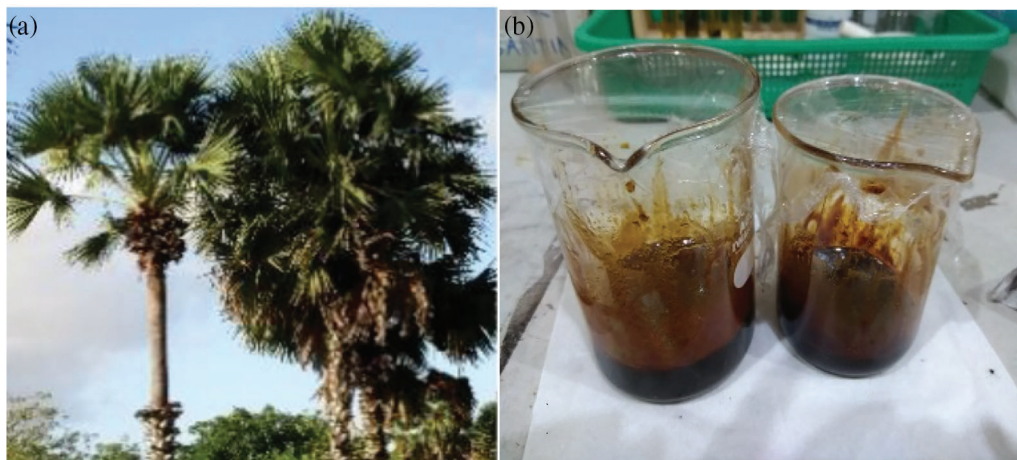


**Figure 1:** (a) Palmyra trees, (b) Thick palmyra sugar

Meanwhile, the  $a\text{-C:N}$  powder is prepared by mixing  $a\text{-C}$  powder with ammonium hydroxide ( $\text{NH}_4\text{OH}$ , Merck 25%) at an  $a\text{-C}$  with an  $\text{NH}_4\text{OH}$  mole ratio of 1:0.066. The mixture is heated using a hotplate at  $150^\circ\text{C}$  and stirred with a magnetic stirrer at 200 rpm for 120 min. Moreover, the  $a\text{-C}$  solution is prepared by mixing 2 g of  $a\text{-C}$  powder with 10 ml of dimethyl sulfoxide ( $\text{DMSO}$ , Merck 99.9%), which is used as a solvent in addition to 10 ml of distilled water. The solution is heated at  $100^\circ\text{C}$ , stirred with a magnetic stirrer at 1500 rpm for 60 min, and exfoliated using ultrasonic for 30 min. It is rotated at 3500 rpm for 30 min using a centrifuge of 80-2 to separate large carbons. It is also important to note that the  $a\text{-C:N}$  solution is prepared using the same process used for the  $a\text{-C}$  solution.

To obtain the characteristic of each layer, thin film deposition of  $a\text{-C}$  and  $a\text{-C:N}$  was carried out on a  $2 \times 2 \text{ cm}^2$  ITO glass substrate. Furthermore, the junction sample is deposited on a  $2 \times 1 \text{ cm}^2$  ITO glass substrate using a nano-sprayer (30 ml USB handy nano mist sprayer Fig. 2a) while the  $a\text{-C/a-C:N}$  junction samples are deposited on size of  $1 \times 1 \text{ cm}^2$  as illustrated in Fig. 2b. The thin film deposition process begins by inserting solution  $a\text{-C}$  and  $a\text{-C:N}$  into the solution container. Before the solution is deposited on the surface of the substrate, several steps occur. These stages are the process of atomization of the solution, flight of droplets to the surface of the substrate, contact of droplets with the surface of the substrate, dispersion and evaporation. The atomizer or nebulizer is intended to form very fine granules from the solution. These very fine granules are accelerated by applying pressure or a high-velocity flow of gas. The very finest of granules are pushed out through the outlet hole and fly to the surface of the substrate. This process occurs inside the nano-sprayer device and occurs shortly after the switch is turned on. The very fine grains directed towards the surface of the substrate form a lamellar layered precipitate. Only grains of the order one nanometer can exit the outlet hole. The grain size greatly determines the quality of the layer formed. The deposition process ends shortly after the switch is turned off. The evaporation process in the atmosphere and contamination from the surrounding environment is protected. This process is carried out within 3 days and a thin film is obtained on the ITO glass substrate. Each layer is deposited within 10 s and the distance between the substrate and solution outlet hole on the nano-sprayer is 5 cm. The sample of the  $a\text{-C/a-C:N}$  junction is carried out by first depositing the  $a\text{-C/N}$  on an ITO glass substrate. After the drying process is complete, the  $a\text{-C}$  layer is deposited on top as illustrated in Fig. 2b.

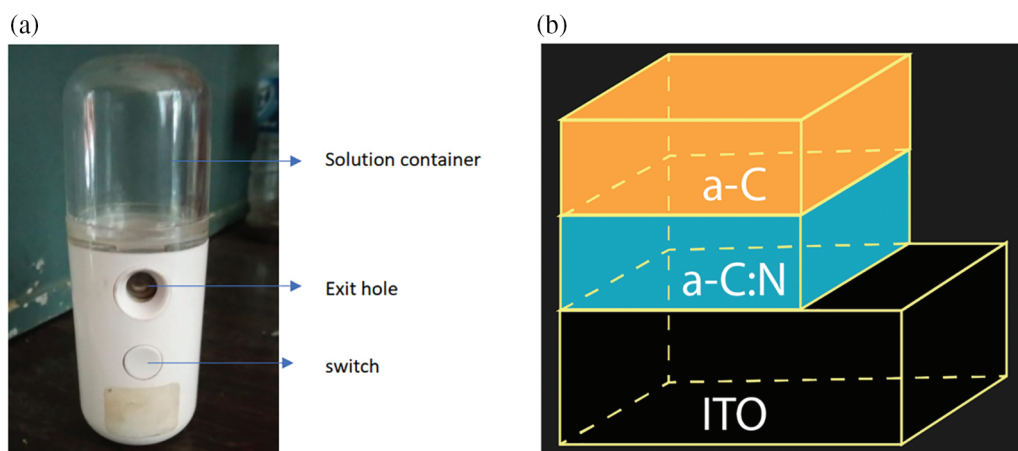


**Figure 2:** (a) Nano-sprayer, (b) Illustration of a sample on a glass ITO substrate

## 2.2 Characterization of Each Layer

The electronic properties and the structure of each layer are important components that influence the characteristics of the junction sample. *XRD* (Philip X' Pert MPD with *Cu Ka* radiation and diffraction angle in the range  $10^{\circ}$ – $60^{\circ}$ ) analysis showed that *a-C* and *a-C:N* layers were in the amorphous phase. Moreover, the electronic and optical properties of the coating greatly affected the junction characteristics of the sample. It was also discovered that the sample could function as a solar cell when each layer has semiconductor electronic properties and an optical energy gap that allows the formation of electron-hole pairs in the visible light region. The electrical conductivity and optical energy gap of each layer obtained using the 4-point probe and UV-Vis spectroscopy (*GENESIS 10 S* with a wavelength in the range of 400–1000 nm) analyses are presented in [Table 1](#). The current and voltage in each layer were discovered to have a linear relationship (ohmic contact).

**Table 1:** Properties of each layer

Layer	Properties		
	Electrical conductivity (S/cm)	Optical energy gap (eV)	Thickness (nm)
<i>a-C</i>	5.5	1.71	262.3
<i>a-C:N</i>	5.6	1.51	197.3

The results of measuring the transmission properties of amorphous carbon (*a-C*) and nitrogen-doped amorphous carbon (*a-C:N*) thin film are shown in [Fig. 3a](#). It can be seen that the transmission properties of light show an increasing value with increasing wavelength. The maximum transmittance value occurs at a wavelength of 900 nm with an energy  $\sim 1.3$  eV. This wavelength is the near-infrared region. So amorphous carbon and nitrogen-doped amorphous carbon film exhibit transparent properties in the region  $\sim 1.3$  eV, characterized by a transmittance value of around 100%. The value of the optical gap energy of *a-C* and *a-C:N* films can be calculated using the *Tauc* formula. The value is obtained by extrapolation as shown in [Fig. 3b](#).

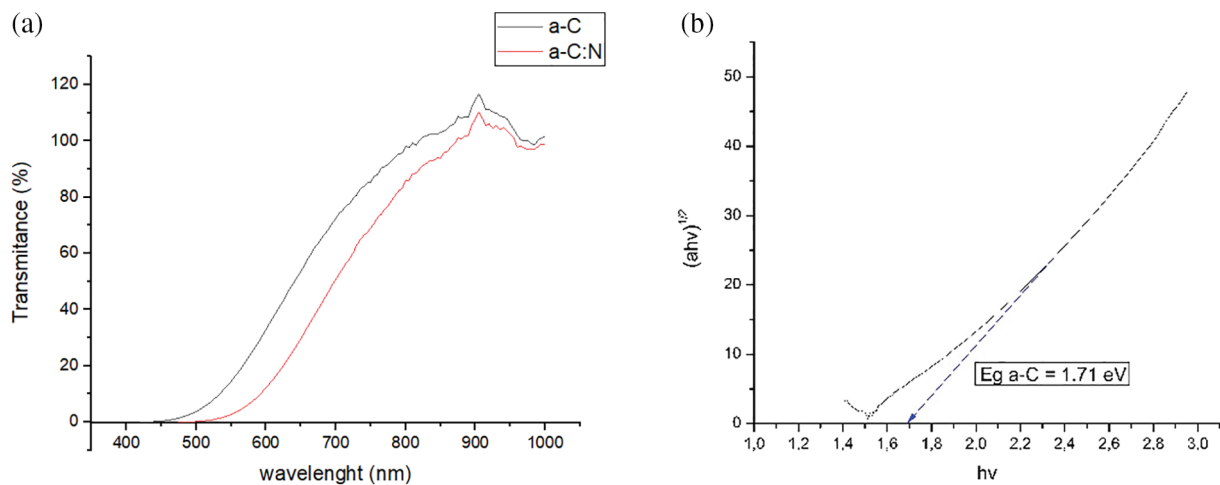


**Figure 3:** UV-Vis measurement results. (a) Transmittance *a-C* and *a-C:N* films. (b) Optical gap energy calculation using Tauc extrapolation

The surface morphology of each layer was determined through the Scanning Electron Microscope (*SEM ZEISS EVO 10*) while the structure was evaluated using the photoemission spectroscopy (*Syn. PES* at beam line 3.2a in the Synchrotron Light Research Institute/*SLRI* Thailand facility). Mode *XPS* under ultra-high vacuum ( $<1 \times 10^{-5}$  Pa) and photon energy in the range 40 to 600 eV, and the results are presented in Fig. 4. The particles in *a-C* and *a-C:N* were observed to be in the order of hundreds of nanometers. The *PES* test was further reviewed on the *C1s* of *a-C* and *a-C:N* layers dominated by  $sp^2$  hybridization and *C-N* bonds, and the formation of *C-N* bonds indicated the possibility of doping and defect processes.

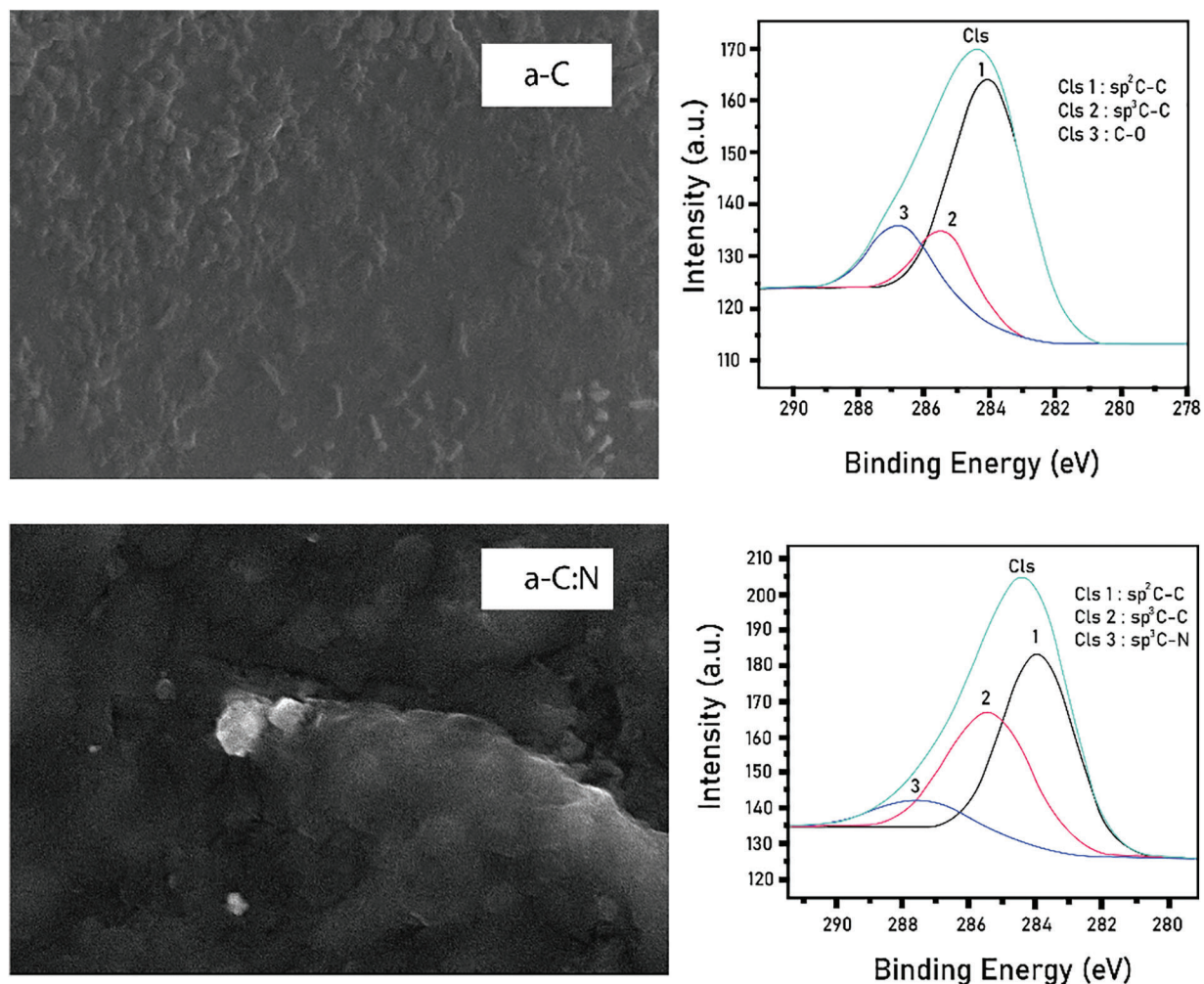


**Figure 4:** Morphology and structure of each layer

The results of the *PES* analysis conducted on the *N1s* spectra are shown in Fig. 5. It was discovered that the spectrum can be deconvoluted into three main components which include *Pyridinic-N* with 398.83 eV [reference  $398.5 \pm 0.1$ ], *Pyrrolic-N* with 399.93 eV [reference  $400.2 \pm 0.1$ ], and *Graphitic-N* with 400.893 eV [reference  $401.2 \pm 0.1$ ]. It is also important to note that the *C-N* bond is a doping process that involves the replacement of a *C* atom by an *N* atom. In the *graphitic-N*, the *C* atoms were replaced by *N* atoms, and this caused doping while a defect was found in *pyrrolic-N* and *pyridinic-N*, which led to the absence

of the doping process [30]. The formation of *graphitic-N* allowed the *a-C:N* to become an *n-type* semiconductor while the *a-C* layer has an intrinsic conduction type. Furthermore, the deconvolution of the *N1s* spectrum in the *a-C:N* layer produced 41.9% *pyridinic-N*, 39.6% *pyrrolic-N*, and 18.5% *graphitic-N*.

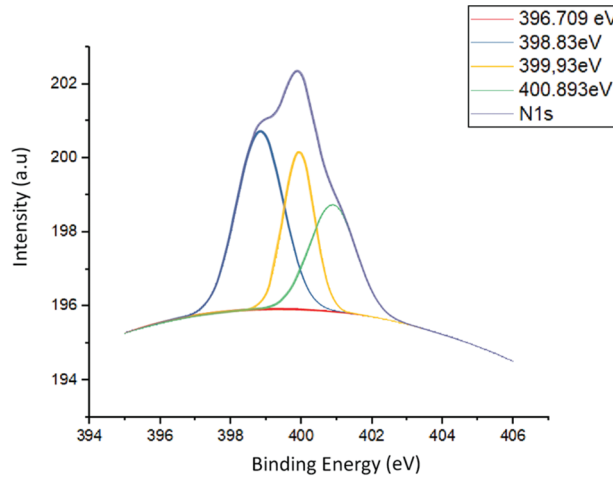


**Figure 5:** Deconvolution of *N1s* spectrum

### 3 Results and Discussion

#### 3.1 Characterization Sample

A solar cell is a photodiode in principle, which means that the junction of two semiconductor materials having different types of conduction is required to comply with the basic rules of a diode required to function as a rectifier. The diode characteristics of the *a-C/a-C:N* junction sample were determined by measuring the current and voltage. The measurement results are presented in the graph in Fig. 6. It was discovered that the relationship between the two indicators meets the rules required or the sample to function as a rectifier. This strengthens the results of testing using *PES* which shows the occurrence of the doping process and *a-C:N* has a different conduction type than *a-C*. These results proved that *a-C* is *intrinsic i* while *a-C:N* is an *n-type*. The results of the current and voltage test provide evidence that rectifier diodes can be made from materials other than silicon. Carbon from biomass can be used as the active material for diodes with cheaper, easier and simpler manufacturing technology. The *a-C/a-C:N* junction is an *i-n* junction diode with a reverse bias current of 127.7 *nA*, a forward bias voltage of 3.3 *mV*, and a breakdown voltage of -3.95 *mV*.

The diode function as a photodiode is characterized by the difference in current and voltage values when in dark conditions compared to bright conditions. The sample functioning as a photodiode is tested by comparing the current and voltage value in the sample when it is dark compared to the value when the sample is illuminated with 1660 lux light. The results of measuring the current and voltage values when dark and when it is illuminated with 1660 lux light are shown in Table 2. The results presented in Table 2 showed an increase in the value of current and voltage when the sample was exposed to light compared to the dark. This shows that the sample functions as a photodiode and has the potential to also function as a photovoltaic cell.

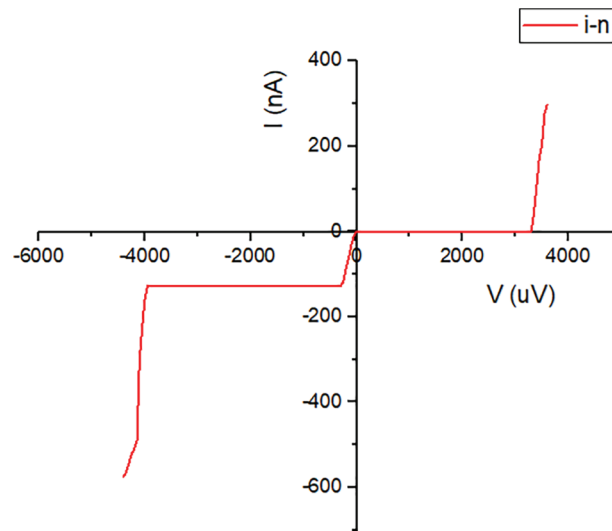


**Figure 6:** I-V curve of a-C/a-C:N junction

**Table 2:** Current and voltage when dark and light

Condition	Current ( <i>nA</i> )	Voltage ( <i>V</i> )
Dark	136	0.14
Light	352	0.35

Whether the sample functions as a photovoltaic cell is found out by measuring the current and voltage values when the sample is exposed to visible light, current and voltage values were measured when the sample was exposed to visible light from lamps with an input power  $2.28$  and  $4.44 \text{ m W/cm}^2$ , and exposure to direct sunlight at *AM 1.5* condition. The relationship between current and voltage when the sample is exposed to visible light from the lamp is shown in Fig. 7. The curve in Fig. 7 shows that the relationship between current and voltage fulfills the rules for the occurrence of the photovoltaic effect. The characteristic values from photovoltaic cells when exposed to light from a lamp are shown in Table 3. Table 3 shows an increase in short circuit current ( $I_{SC}$ ) and open circuit voltage ( $V_{OC}$ ) with increasing emitted light power. The increase in  $I_{SC}$  and  $V_{OC}$  values does not seem to be directly proportional to the input power. This can be seen when the input power is increased two times; the increase in  $I_{SC}$  and  $V_{OC}$  values is not two times either.

The sample was also exposed to direct sunlight at *AM 1.5* ( $100 \text{ m W/cm}^2$ ), and the relationship between the current and the generated voltage is presented in Fig. 8. It was discovered that the relationship also fulfills the requirement for the emergence of the photovoltaic effect.

This proves that the junction sample is a photovoltaic cell because the electron in the valence band of the type i layer receives sufficient energy to be excited toward the conduction band when the sample is exposed to light to become a free electron and leave a hole in the valence band. This causes the type i layer to have an excess of holes. Meanwhile, light exposure in the n-type layer is able to excite an electron from the valency band to the conduction band to become a free electron and the n layer has excess electrons. The hole in the i layer is unable to diffuse to the n-type because it is blocked by the built-in electric field in the depletion layer

while the electron passes through the depletion region toward the n-type layer. It is important to note that the electron flows toward the external resistance. However, the hole in the n-type breaks through the depletion region to the type-i region and flows into the external resistance. This means the holes and electrons flow into the external circuit as an electric current to create a potential difference across the external resistance. The current and voltage in this external circuit were found to be the benchmarks for the output power of the solar cell sample. This shows that the electron-hole pairs arose when exposed to light in the *a-C/a-C:N* junction sample, indicating its ability to function as a solar cell. The ability of the sample to function as a solar cell depends highly on the current flowing in the external circuit. It was discovered that the short circuit current ( $I_{SC}$ ) and open circuit voltage ( $V_{OC}$ ) increased when it was exposed to direct sunlight. The maximum current and voltage in the curve presented in Fig. 8 were used to calculate the photovoltaic characteristics of the junction sample, and the results obtained are listed in the following Table 4. The table shows that the sample functions as a solar cell with a maximum efficiency of 0.0013%. In Table 4, it can be seen that the  $I_{SC}$  is still too small compared to  $V_{OC}$ . There is a possibility of a recombination process immediately after the generation of an electron and a hole after the sample is exposed to light. The reason for the recombination is probably that the thickness of each layer of the spliced sample is not optimal. It is still too thin. The second probability is caused by a defect in the *a-C:N* layer, which is characterized by the formation of *Pyridinic-N* and *pyrrolic-N* compounds.

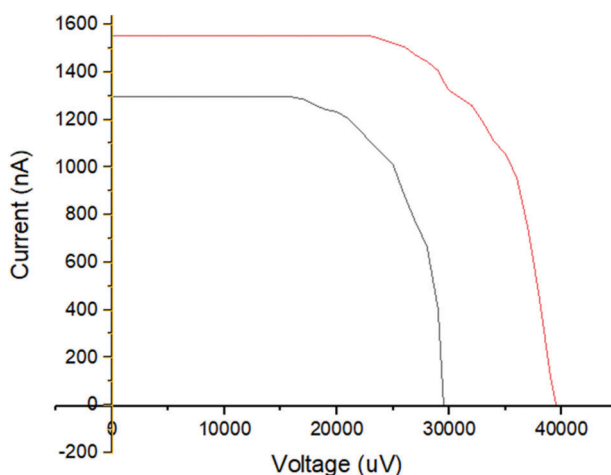


**Figure 7:** I-V curve on exposure to light

**Table 3:** Characteristic photovoltaic

Characteristics photovoltaic	Input power ( $m W/cm^2$ )	
	2.28	4.44
$I_{SC}$ (nA)	1297	1553
$V_{OC}$ ( $\mu V$ )	29.500	39.500

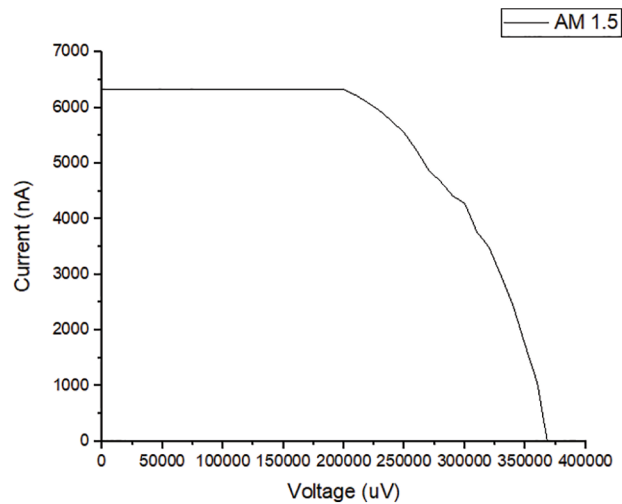


**Figure 8:** The curve of the relationship between current and voltage *AM 1.5* conditions

**Table 4:** Characteristics of the photovoltaic sample

Properties of photovoltaic sample	value
$I_{SC}$	6320 nA
$V_{OC}$	363300 $\mu V$
$I_{max}$	5936 nA
$V_{max}$	230000 $\mu V$
Fill Factor	58.65%
Efficiency	0.0013%

This research is initial research on the development of solar cells using a biomass source. The developed solar cell is an amorphous carbon homojunction that has not been developed by previous researchers. Previous development of carbon-based solar cells was dominated by heterojunction between carbon and silicon. The deposition method using *CVD*. The doping source is generally used as the gas source. In this research, the n-type layer doping source was used, namely ammonium hydroxide ( $NH_4OH$ ) in liquid form. The doping process is carried out very simply, easily and at a very low cost. As a comparison, the price of  $NH_4OH$  of ~5 US \$ per liter is much cheaper than that of nitrogen gas. The deposition method in this research used a nano-sprayer, which had a price of less than 10 US \$. It is much cheaper compared to *CVD*, which has a price of over one million US \$. As a comparison, the results of this research along with similar research conducted by previous researchers are shown in [Table 5](#).

**Table 5:** Comparison with the results of previous research

Researcher	Configuration	Source	Method	Efficiency (%)
Fadzilah [26]	<i>a-C/p-Si</i>	Camphor oil	<i>AACVD</i>	0.000048
<b>This research</b>	<b><i>a-C/a-C:N/ITO</i></b>	<b>Palmyra sugar</b>	<b>Nano-spraying</b>	<b>0.0013</b>

It can be seen in Table 5 that the resulting efficiency increased by two digits compared to that produced by a previous researcher with a similar configuration and different method. This shows that the development of solar cell technology using biomass sources and the nano-spraying method produces better results than the CVD method in a similar configuration. The use of local materials as active materials for solar cell development with this method provides added value to the simplicity of the method, availability of raw materials, low cost and environmentally friendly. Currently, the author and team have developed a solar cell with the same method and materials with the configuration  $a-C:B/a-C:N/ITO$  and  $a-C:B/a-C/a-C:N/ITO$  and have achieved an efficiency value of  $\sim 1\%$  and have not yet been published. In subsequent development research, the author and team continue to develop efficiency optimizations produced in the  $a-C:B/a-C/a-C:N/ITO$  configuration with a target of achieving an efficiency value of 15% in the next 3–5 years and the capability of commercialization.

#### 4 Conclusions

The  $a-C/a-C:N$  junction sample was successfully deposited through an  $i-n$  junction diode to act as a *rectifier*. It was discovered that the current and voltage values increased when exposed to visible light. This indicates the creation of an electron-hole pair and also shows that the sample is a photodiode. Moreover, the relationship between the current and voltage when illuminated with visible light and directly under sunlight satisfied the photovoltaic cell requirement, and this means the sample can be used as a solar cell with a maximum efficiency of 0.0013%. The liquid palmyra sugar used as the carbon source also shows the possibility of developing solar cells using renewable carbon-active materials. Furthermore, the simple nano-sprayer deposition method applied indicates the potential for developing solar cells through green, inexpensive, easy, and renewable technology.

**Acknowledgement:** The authors highly appreciate SLRI (public organization) Thailand for providing the PES facilities used in this research. The authors appreciatively acknowledge the Research Council of the University.

**Funding Statement:** This research was partly funded by the University of Muhammadiyah Malang through a doctoral scientific work development program and also by the Ministry of Finance of Indonesia through the LPDP BUDI-DN scholarship (BP), and National Competitive Fundamental Research Grant (Hibah Penelitian Dasar), Kemendikbudristek, 2021–2022 (D).

**Author Contributions:** All authors contributed to the process of fabricating, measuring and writing the manuscript.

**Availability of Data and Materials:** The data that support the findings of this study are openly available in the following sources: Key Engineering Materials (2020), Vol. 860, pp. 185–189. <https://doi.org/10.4028/www.scientific.net/KEM.860.185>; Key Engineering Materials (2020), Vol. 860, pp. 190–195. <https://doi.org/10.4028/www.scientific.net/KEM.860.190>; Key Engineering Materials (2020), Vol. 860, pp. 196–201. <https://doi.org/10.4028/www.scientific.net/KEM.860.196>; Journal Renewable Materials (2021), Vol. 9, No. 6, pp. 1087–1098. <https://doi.org/10.32604/jrm.2021.014466>.

**Conflicts of Interest:** The authors declare that they have no conflicts of interest to report regarding the present study.

#### References

1. Robertson, J. (2002). Diamond like amorphous carbon. *Materials Science and Engineering: R: Reports*, 37(4–6), 129–281.
2. Furlan, K. P., Klein, A. N., Hotza, D. (2013). Diamond like carbon films deposited by hydrocarbon plasma sources. *Review Advanced Materials Science*, 34, 165–172.

3. Zhu, J., Li, F., Liu, G., Liu, D., Li, Q. et al. (2018). Synthesis of amorphous carbon film in ethanol inverse diffusion flames. *Nanomaterials*, 8(9), 656.
4. Li, Z., Cui, C., Zhou, X., Bian, S., Arteaga, O. et al. (2022). Characterization of amorphous carbon films from 5 nm to 200 nm on single-side polished a-plane sapphire substrates by spectroscopic ellipsometry. *Frontier in Physics*, 10, 965. <https://doi.org/10.3389/fphy.2022.968101>
5. Kyle, D. A., Wegener, G., Matthew, D. S., Robert, J. B., Feng, X. et al. (2021). Biogenic formation of amorphous carbon by anaerobic methanotrophs and select methanogens. *Science Advances*, 7(44), eabg9739. <https://doi.org/10.1126/scisdv.abg9739>
6. Neustroev, E. P., Prokopyev, A. R., Semenov, S. O., Popov, V. I., Protopopov, F. F. et al. (2021). Research of properties of a carbon film formed in methane plasma and the following annealing. *IOP Conference Series: Materials Science and Engineering*, 1079, 042086. <https://doi.org/10.1088/1757-899X/1079/4/042086>
7. Zhai, Z., Shen, H., Chen, J., Li, X., Jiang, Y. (2018). Evolution of structural and electrical properties of carbon films from amorphous carbon to nanocrystalline graphene on quartz glass by HFCVD. *ACS Applied Materials & Interfaces*, 10(20), 17427–17436. <https://doi.org/10.1021/acsami.8b01588>
8. Chen, L., Wei, X., Zhang, G., Shang, L., Lu, Z. et al. (2021). Probing the tribological performances of hydrogenated amorphous carbon film in methane atmosphere based on Hertzian elastic contact model. *Tribology International*, 155, 106790.
9. Shinohara, M., Tominaga, T., Shimomura, H., Ihara, T., Yagyu, Y. et al. (2019). Deposition of hydrophilic amorphous carbon film with ether as a source molecule and analysis of its deposition reaction. *Electronic and Communication in Japan*, 102(4), 3–9.
10. Hamdan, A., Makdessi, A. G., Margot, J. (2016). Synthesis of amorphous hydrogenated carbon thin films by magnetized radio-frequency discharge in argon-acetylene mixture at very low gas pressure. *Thin Solid Films*, 599, 84–97.
11. Kamrul, H. M., Kumar, P. B., Hatta, A. (2006). Electrical resistivities of the diamond like carbon films fabricated from methane and acetylene using RF plasma. *New Diamond and Frontier Carbon Technology*, 16(4), 211–219.
12. Ishak, A., Nurrisal, M. A., Rusop, M. (2015). Optical properties of as-deposited amorphous carbon film from various substrate temperatures via custom-made CVD. *International Journal of Scientific and Technology Research*, 4(1), 257–261.
13. Ishak, A., Rusop, M. (2014). Physical properties of nitrogen doped amorphous carbon films from ethanol precursor for solar cell applications. *International Journal of Scientific and Technology Research*, 3(10), 309–312.
14. Pamungkas, D. I., Haikal, A., Bagiya, M. A., Cahyono, Y., Darminto. (2018). Synthesis of amorphous carbon from bio-product by drying method. *AIP Conference Proceeding*, 1945(1), 020059.
15. Pamungkas, D. I., Mukarromah, Priyanto, B., Nakajima, H., Tunmee, S. et al. (2019). Structural analysis and electrical properties of amorphous carbon thin films. *Materials Science Forum*, 966, 66–71.
16. Mukarromah, I., Darminto, D. P. (2019). Structural characterization of amorphous carbon films from palmyra sap. *AIP Conference Proceeding*, 2120(1), 050011.
17. Resplendi, F., Bernardi, M., Cicero, G., Grossman, J. C. (2014). Structure-property relation in amorphous carbon for photovoltaic. *Applied Physics Letter*, 105, 043903.
18. Debajyoti, D., Banerjee, A. (2015). Anti-reflection coatings for silicon solar cells from hydrogenated diamond like carbon. *Applied Surface Science*, 345, 204–215.
19. Addie, A. J., Raid, A. I., Mudhafar, A. M. (2022). Amorphous carbon nitride dual-function anti-reflection coating for crystalline silicon solar cells. *Scientific Report*, 12(1), 1–12.
20. Oliviera, Jr. M. H., Silva, D. S., Cortes, A. D. S., Namani, M. A. B., Marques, F. C. (2009). Diamond like carbon used as anti-reflective coating on crystalline silicon solar cells. *Diamond & Related Materials*, 18, 1028–1030.
21. Teixeira, C. O., Andrade, L., Mendes, A. (2019). Novel carbon-based material for perovskite solar cells back-contact. *International Journal of Energy Research*, 43(13), 7541–7546.
22. Bogachuk, D., Tsuji, R., Martineau, D., Narbey, S., Herterich, J. P. et al. (2021). Comparison of highly conductive natural and synthetic graphite foe electrodes in perovskite solar cells. *Carbon*, 178, 10–18.

23. Adhikari, S., Kayastha, M. S., Ghimire, D. C., Aryal, H. R., Adhikary, S. et al. (2013). Improved photovoltaic properties of heterojunction carbon based solar cell. *Journal of Surface Engineered Materials and Advanced Technology*, 3, 178–183.
24. Khan, R. U. A., Silva, S. R. P., Van Swaij, R. A. C. M. M. (2003). Polymeric amorphous carbon as p-type window within amorphous silicon solar cells. *Applied Physics Letter*, 82(22), 3979–3981.
25. Ahmad, N., Kamaruzzaman, D., Rusop, M. (2012). Amorphous carbon deposited by novel aerosol assisted chemical vapor deposition for photovoltaic solar cells. *Japanese Journal of Applied Physics*, 51(6S), 06FD05.
26. Fadzilah, A. N., Dayana, K., Rusop, M. (2012). Carbon-based solar cell from amorphous carbon with nitrogen incorporation. *Advanced Materials Research*, 576, 785–788.
27. Zhao, X., Wu, H., Yang, L., Wu, Y., Sun, Y. et al. (2019). High efficiency CNT-Si heterojunction solar cells by dry gas doping. *Carbon*, 147, 164–171.
28. Eguchi, T., Kato, S., Kishi, N., Soga, T. (2022). Effect of thickness on photovoltaic properties of amorphous carbon/fullerene junction. *AIMS Materials Science*, 9(3), 446–454.
29. Soga, T., Nakagaki, T., Kato, S., Kishi, N. (2018). Effect of sublimation of temperature on the photovoltaic properties of amorphous carbon thin film from fullerene. *Journal of Solar Energy Research Update*, 5, 8–13.
30. Wei, D., Liu, Y., Wang, Y., Zhang, H., Huang, L. et al. (2009). Synthesis of N-doped graphene by chemical vapor deposition and electrical properties. *Nano Letter*, 9(5), 1752–1758.